Received: 14 January 2025 | Revised: 13 March 2025 | Accepted: 18 April 2025 | Published online: 9 May 2025

RESEARCH ARTICLE

Journal of Optics and Photonics Research
2026, Vol. 3(2) 140–145
DOI: 10.47852/bonviewJOPR52025210

BON VIEW PUBLISHING

Dependence of the Electromagnetic Radiation Transmission Coefficient of Liquid Crystal π – Cells in the Terahertz Range

Anfal Fadhil Ahmed Mulamahawsh[1] and G. V. Simonenko[1,*]

[1]*Saratov National Research State University named after N.G. Chernyshevsky, Russia*

Abstract: In this article, a modified Abeles technique is proposed for calculating the energy transmission coefficient of electromagnetic radiation of a liquid crystal modulator operating on the basis of a π-cell. The proposed technique has an accuracy of modeling the characteristics of the liquid crystal modulator comparable to known analogs. The results of computer modeling allow us to draw the following practical conclusions. The effect of changing the design parameters on the transmission coefficient of the liquid crystal modulator increases with a decrease in the wavelength of the electromagnetic range within the range from 16 μm to 1 μm. The maximum effect on the transmission coefficient of the liquid crystal modulator in the short-wave part of electromagnetic radiation is exerted by the thickness of the electrode layer, while there is no such dependence in the long-wave part of this radiation. The thickness of the orienting layer of the liquid crystal modulator has the same effect on its transmission coefficient as the thickness of the electrode layer, but with a smaller amplitude. The control voltage of the liquid crystal modulator has a significant effect on its transmission coefficient of electromagnetic radiation for short wavelengths and almost does not affect it in the long-wave region of electromagnetic radiation.

Keywords: liquid crystal, modulator, transmission coefficient, matrix method

1. Introduction

Currently, the use of terahertz radiation has found wide application in the field of communications and diagnostics of various environments, including biological structures [1, 2]. This process has been facilitated by significant developments in the technologies for generating and detecting terahertz waves [3, 4]. Further development of technologies of the terahertz range of electromagnetic waves requires the development of various devices for controlling this radiation [5, 6]. Currently, various devices based on graphene, pin diodes, and liquid crystals (LC) are used for these purposes [7–12]. From the point of view of control systems, the most attractive are LCs, as they provide stable operation, low energy losses, and smooth changes in their dielectric properties [13–15]. It should be noted that LCs are often used in photonics to provide tuning of integrated optical devices due to their unique electro-optical properties. LCs have various properties such as high birefringence, significant electro-optical effect, low excitation power, and low-power consumption, which makes them a promising material for the implementation of low-power tunable waveguide components and devices [16]. Recently, liquid crystal devices (LCDs) have been used in various optical devices such as optical filters, attenuators, switches, and laser beam control devices [17–21]. The most common applications of LCDs are in various optical devices such as displays, attenuators, tunable polarizers, spatial light modulators, optical switches, filters, biosensors, radiation detectors, etc. [22, 23]. For these purposes, the same ones as nematics are most often used [24, 25]. In this regard, the authors of this article proposed an original design of an LC modulator based on the simultaneous use of several π-cells [26], the use of which raises the question of minimizing losses due to multi-wave interference in the layered structure of such a device. This work is devoted to studying this issue.

2. Method of Modeling the Transmission Coefficient of an LC Cell

Usually, various matrix methods based on the Jones or Berreman matrix formalism are used to model the optical characteristics of LC modulators of electromagnetic radiation [27, 28]. In addition, well-known software packages are used to calculate the characteristics of such devices only in the visible range of electromagnetic radiation [27, 28]. The calculation method of optical characteristics of LC modulators based on Jones matrices does not allow taking into account the phenomenon of multi-wave interference in its multilayer structure. At the same time, the Berreman matrix method correctly takes into account this phenomenon, but requires a large number of calculations. To eliminate these shortcomings, we propose using the Abeles matrix method [29]. To correctly apply this method, we will introduce several practically justified assumptions: (1) most often such devices are used in conditions where the modulated radiation propagates through it parallel to the normal to the modulator surface [28], (2) the basis of the modulator is a LC cell, which is filled with a nematic with a zero-twist angle of the LC structure. These two restrictions allow us to assume that if the modulator is exposed to

*Corresponding author: G. V. Simonenko, Saratov National Research State University named after N.G. Chernyshevsky, Russia. Email: simonenkogv@sgu.ru

© The Author(s) 2025. Published by BON VIEW PUBLISHING PTE. LTD. This is an open access article under the CC BY License (https://creativecommons.org/licenses/by/4.0/).

Figure 1
The structure of a standard LC cell, on the basis of which the radiation modulator operates

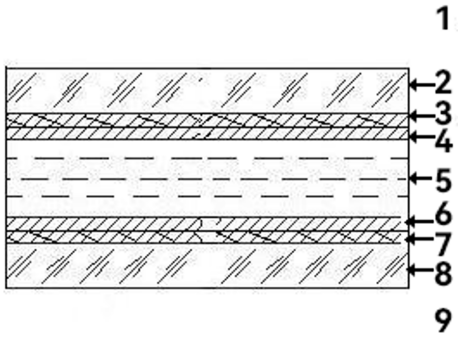

o- or e-type radiation, then this type of polarization is preserved. O – polarization type is a linearly polarized electromagnetic wave whose electric field vector is perpendicular to the optical axis of the LC. E – polarization type is a linearly polarized electromagnetic wave whose electric field vector is parallel to the optical axis of the LC.

If the modulated radiation is not polarized, the LC cell is placed between two crossed polarizers. If the initially modulated radiation is linearly polarized, the input polarizer is missing. Note that the radiation is modulated due to the effect of electric field-controlled double refraction [28, 30]. In this case, the maximum transmittance (transmission coefficient) of electromagnetic radiation transverse magnetic (TM) is determined by the amount of loss due to multi-wave interference in the layered structure of the device. In Figure 1, the classical design of such an LC modulator is presented. Let us consider the propagation of a linearly polarized electromagnetic wave in such a structure at an incidence angle of 0°. In the LC cell, two waves (ordinary and extraordinary) will propagate in the forward direction and two in the opposite direction. In this case, the polarization type of the wave propagating in this cell will not change, since the radiation propagates along the normal to the cell surface, and the twist angle of the LC structure is 0°. Therefore, we can first calculate the transmission coefficient of the ordinary wave (o-type) in such a system and then for the extraordinary wave (e-type). The transmission coefficient of the total radiation can be obtained by incoherently adding the ordinary and extraordinary waves.

Let E_o^+, E_{or}^-, E_{ot}^+ – be the complex amplitudes of the electric field vectors of the electromagnetic waves of the o-type incident on the LC cell, reflected from it, and transmitted through it, respectively. Similarly, E_e^+, E_{er}^-, E_{et}^+ – are the complex amplitudes of the electric field vectors of the electromagnetic waves of the e-type incident on the LC cell, reflected from it, and transmitted through it. Then, the amplitudes of all ordinary and extraordinary waves are related by the known relation [29]:

$$\begin{bmatrix} E^+_{o(e)} \\ E^-_{o(e)r} \end{bmatrix} = \begin{bmatrix} S_{11} & S_{12} \\ S_{21} & S_{22} \end{bmatrix} \cdot \begin{bmatrix} E^+_{o(e)t} \\ 0 \end{bmatrix} \quad (1)$$

Where:

$$S = \begin{bmatrix} S_{11} & S_{12} \\ S_{21} & S_{22} \end{bmatrix}$$

$$S = I_{01} \cdot L_1 \cdot I_{12} \cdot L_2 \cdot I_{23} \cdot L_3 \cdot I_{34} \cdot L_4 \cdot I_{45} \cdot L_5 \cdot I_{56} \cdot L_6 \cdot I_{67} \cdot L_7 \cdot I_{78} \cdot L_8 \cdot I_{89} \quad (2)$$

$$I_{kj} = \frac{1}{t^{o(e)}_{kj}} \begin{bmatrix} 1 & r^{o(e)}_{kj} \\ r^{o(e)}_{kj} & 1 \end{bmatrix}, L_i = \begin{bmatrix} e^{i\beta^{o(e)}_j} & 0 \\ 0 & e^{-i\beta^{o(e)}_j} \end{bmatrix}, r^{o(e)}_{kj} = -\frac{n^{o(e)}_j - n^{o(e)}_k}{n^{o(e)}_j + n^{o(e)}_k}$$
$$t^{o(e)}_{kj} = \frac{2n^{o(e)}_k}{n^{o(e)}_k + n^{o(e)}_j}, \beta^{o(e)}_j = \frac{2\pi l_j n^{o(e)}_j}{\lambda}, i = 1, ..., 8, k = 0, ..., 8, j = 1, ..., 9 \quad (3)$$

$$n^e_5 = \frac{1}{l_5} \int_0^{l_5} \left(\frac{n_e \cdot n_o}{\sqrt{n_o^2 \cos^2\theta(x) + n_e^2 \sin^2\theta(x)}} \right) dx, n^o_5 = n_o \quad (4)$$

the values of indices i, j, k correspond to Figure 1; l_i and n_i are the thicknesses and refractive indices of the corresponding media, n_e and n_o are the extraordinary and ordinary refractive indices of the LC; accordingly, λ is the wavelength of the modulated radiation; l_5 is the thickness of the LC layer; x – is the current coordinate of the orientation of the LC director along its thickness; $\theta(x)$ is the orientation angle of the LC director.

1, 9 – external semi-infinite environment: 2, 8 – glass plates: 3, 7 – control electrodes; 4, 6 – orientation layers; 5 – layer of planar oriented nematic with antisymmetric boundary conditions.

Then, the amplitude transmittance coefficient for an electromagnetic wave o – (e –) type $\tau_{o(e)}$ and the corresponding transmission coefficient $T_M^{o(e)}$ are calculated as follows:

$$\tau_{o(e)} = 1/S_{11o(e)}, \; T^{o(e)}_M = \tau_{o(e)} \cdot \tau_{o(e)} \quad (5)$$

If a linearly polarized electromagnetic wave falls on a LC cell and the angle between the polarization direction and the optical axis of the LC is equal to α, then the total transmission coefficient (energy transmittance coefficient) for the electromagnetic wave T_M is determined using the expression:

$$T_M = T^o_M \cos^2\alpha + T^e_M \sin^2\alpha \quad (6)$$

In the case when unpolarized electromagnetic radiation falls on the LC cell or the angle $\alpha = 45°$, then Equation (6) can be rewritten as:

$$T_M = (T^o_M + T^e_M)/2 \quad (7)$$

Thus, using Equations (1)–(7) it is possible to calculate the transmittance of electromagnetic radiation for the T_M, modulator operating on the basis of the "classical" π – cell in a simple way. The algorithm for calculating the TM coefficient of the LC modulator in this case consists of the following steps. In the first step, taking into account the boundary conditions in the LC cell and the physical constants of the LC (elasticity coefficients and dielectric constants), the distribution of the orientation angles of the LC director $\theta(x)$ is calculated at a given control voltage. This problem is not included in the calculation part of the proposed method, but is used from a well-known software package [28]. In the second step, assuming that the LC layer is described by the ordinary refractive index n_o ($n_5 = n_o$), using the Equations (1), (2), (5), we calculate the transmission coefficient of the ordinary wave T_M^o. After this, we assume that the LC layer is described by the average refractive index for the extraordinary wave, and using the Equations (1)–(3), and (5), we calculate the transmission coefficient of the extraordinary wave T_M^e. If a linearly polarized electromagnetic wave falls on the LC cell, the polarization direction of which makes an angle α with the optical axis of the LC, then the total transmission coefficient (transmission coefficient) T_M for the electromagnetic wave is calculated using

Equation (6). In the case when unpolarized electromagnetic radiation falls on the LC cell, the energy transmittance coefficient T_M is calculated using Equation (7).

Based on the described algorithm, a corresponding software tool has been developed for calculating the energy transmittance of the T_M LC modulator operating on the basis of a "classical" π-cell. The following set of LC cell parameters is used to calculate the attenuation (transmittance) coefficient: refractive indices of the medium (n_1, n_9) in which the cell is located; refractive index and thickness of glass substrates (n_2, n_8, l_2, l_8); refractive index and thickness of electrode layers (n_3, n_7, l_3, l_7); refractive index and thickness of orienting layers(n_4, n_6, l_4, l_6); refractive indices of the LC (n_o, n_e) and the thickness of its layer l_5; wavelength λ of modulated electromagnetic radiation and the initial distribution of orientation angles of the LC director.

The level of adequacy of the proposed software tool was determined by comparing the results of modeling the dependences of the transmission coefficients of the T_M LC modulator on the control voltage U, obtained using the proposed method and using the MOUSE-LCD software package [28] for the visible range of electromagnetic radiation. The comparison showed that the discrepancy between these data does not exceed 10%, which corresponds to the accuracy of the calculations of the MOUSE-LCD software package itself and indicates the adequacy of the proposed simple method for calculating the energy transmission coefficient of the π-cell-based LC modulator. Note that the proposed simple method for calculating the transmission coefficient of an LC modulator differs from the "classical" Abeles method in that it allows for multi-beam interference in anisotropic layered media to be taken into account.

3. Results and Discussion

Let us consider the influence of the design parameters of the LC modulator on its characteristics. To exclude the cross-influence of the double refraction effect and the multi-beam interference effect on the characteristics of the device, let us consider the design of the modulator without polaroids. In this case, only the phenomenon of multi-wave interference in the layered structure of the device plays a role, which determines the maximum possible value of the transmission coefficient of the modulator T_M. Let us consider the influence of the design parameters of the LC modulator on its characteristics. To exclude the cross-influence of the double refraction effect and the multi-beam interference effect on the characteristics of the device, let us consider the design of the modulator without polaroids. In this case, only the phenomenon of multi-wave interference in the layered structure of the device plays a role, which determines the maximum possible value of the transmission coefficient of the modulator T_M. The value of this characteristic is significantly influenced by such design parameters of the LC modulator as values of the LC refractive indices (n_e, n_o); thickness of the LC layer; refractive indices; and thicknesses of the orienting and electrode layers [31]. It is worth noting that increasing the thickness of the LC layer significantly worsens the switching dynamics of the LC device [28]. Therefore, we will not consider the effect of this parameter on the transmission coefficient and will fix its value. In studies, it is considered that the thickness of the LC layer is 2 μm. At the same time, standard LC devices use materials with fixed physical parameters as an orientant and electrode layer, in this case, refractive indices. Therefore, the values of these parameters also did not change. On the other hand, the control voltage changes the value of the refractive index for the e-wave from n_e to n_o, which can significantly affect the transmission coefficient of the LC modulator. In view of the above, we selected the following as parameters that can significantly affect the value of the transmission coefficient of the modulator: control voltage U of the modulator; refractive index for the e-wave of the LC; thickness of the electrode layer $d_{elect.}$ thickness of the orienting layer d_{orient}.

This functional multidimensional dependence can be most clearly studied using the following partial derivatives: $T_{MU}^{`} = \partial T_M/\partial U$; $T'_{Mn_e} = \partial T_M/\partial n_e$; $T'_{Md_{electr}} = \partial T_M/\partial d_{electr}$; $T'_{Md_{orient}} = \partial T_M/\partial d_{orient}$. Figures 2–5 show the simulation results. Analysis of these figures shows that changes in the above design parameters

Figure 2

Dependence of the derivative of the transmission coefficient with respect to the voltage of the LC modulator on the control voltage for different wavelengths of electromagnetic radiation

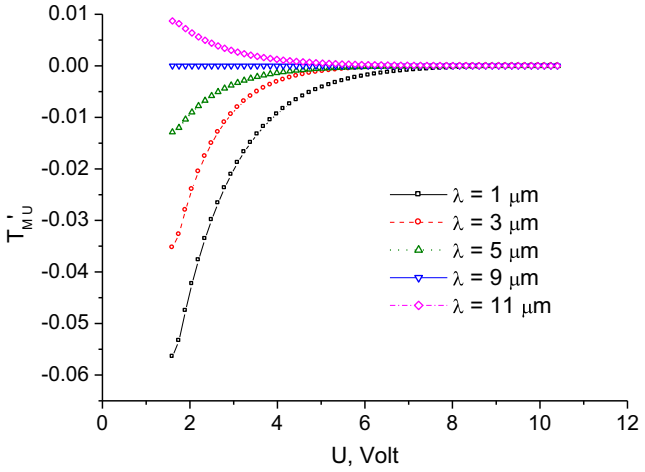

Figure 3

Dependence of the derivative of the transmission coefficient with respect to the refractive index of the extraordinary wave of the liquid crystal on the value of the extraordinary refractive index for different wavelengths of electromagnetic radiation

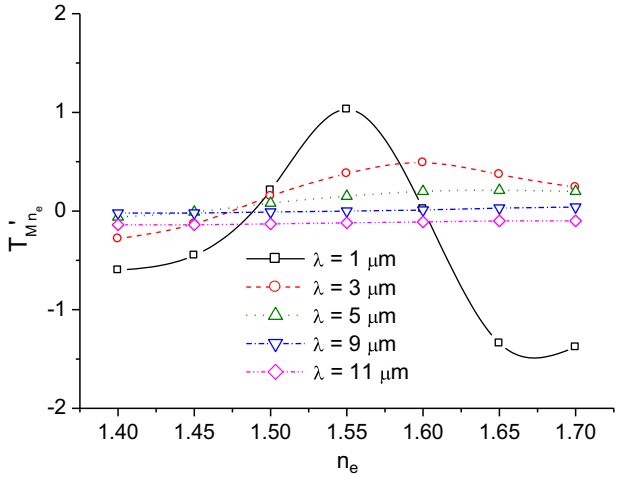

Figure 4
Dependence of the derivative of the transmission coefficient of the LC modulator by the thickness of the electrode layer on the thickness of the electrode layer for different wavelengths of electromagnetic radiation

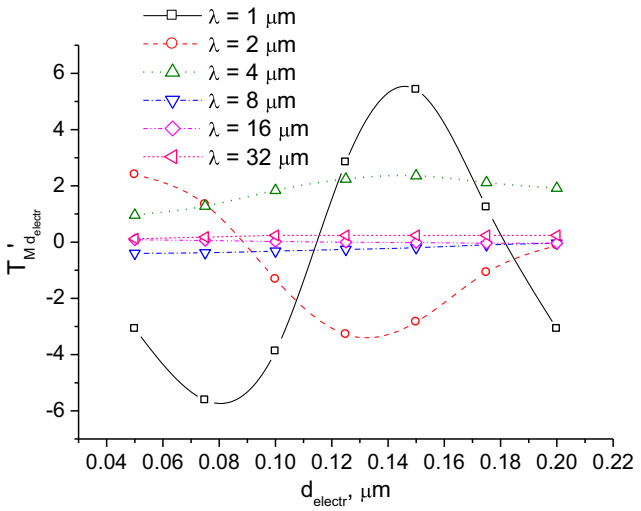

Figure 5
Dependence of the derivative of the transmission coefficient of the LC modulator on the thickness of the orienting layer on the thickness of the orienting layer for different wavelengths of electromagnetic radiation

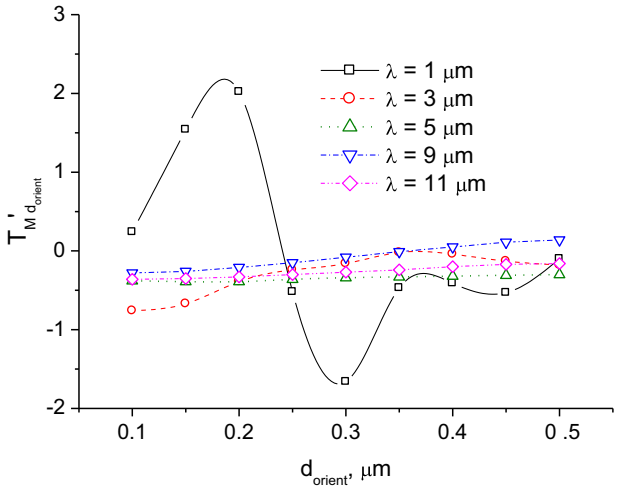

of the LC modulator have a greater effect on the transmission coefficient of the device for shorter wavelengths of electromagnetic radiation. Thus, for radiation with a wavelength of 1 μm, a change in the control voltage in the operating range leads to a sharp change in the derivative of the transmission coefficient with respect to voltage, while for wavelengths of 9 or 11 μm this derivative is almost independent of U (Figure 2).

In this case, the sign of the derivative changes for wavelengths in the ranges from 9 μm to 11 μm. Similar behavior is observed for the dependence on U (Figure 3). This is explained as follows. The value of the derivative of the transmission coefficient with respect to voltage from the modulator control voltage is determined by multi-wave interference in the layered structure of the device. The result of interference in turn depends on the phase parameter Φ ($\Phi = n \cdot l/\lambda$, where n is the refractive index of the medium in which radiation with a wavelength of λ propagates, l is the thickness of the medium in which the radiation propagates) [32]. Changing the control voltage leads to a change in the value of the refractive index of the LC, which entails a change in the phase parameter. For the short-wave part of the electromagnetic radiation spectrum, the changes in the phase parameter are significantly stronger than for the long-wave part. Therefore, the T_{Mn_e} dependences in the short-wave part of the radiation spectrum are more clearly expressed than in the long-wave part of the spectrum. It is worth noting the correspondence of the curves shown in Figures 2 and 3 in the region where n_e changes from 1.5 to 1.6.

If we consider the dependence of the transmission coefficient of the LC modulator on the thickness of the electrode (d_{electr}) and orienting (d_{orient}) layers, then their nature is similar to the two previous dependencies (Figures 4 and 5). That is, T_M for small λ strongly depends on d_{electr} and d_{orient} and with increasing wavelength of electromagnetic radiation this dependence weakens. The explanation for such behavior of the dependencies $T'_{Md_{electr}}$ and $T'_{Md_{orient}}$ is similar to that written above for T_{MU}' and T'_{Mn_e}. The differences are that the changes in the parameters d_{electr} and d_{orient} occur several times, and the change in the parameter n_e– is only no more than 25%. At the same time, the change in the modulator control voltage occurs in a very wide range, but this change causes a decrease in n_e from the maximum value to the minimum and does not exceed 30%. Therefore, the $T_M(d_{electr})$ and $T_M(d_{orient})$ dependencies in the short-wave part of the electromagnetic radiation spectrum have a more pronounced character than the dependencies T_M (U) and $T_M(n_e)$.

4. Conclusion

This article proposes a modified Abeles method for calculating the transmission coefficient of electromagnetic radiation of an LC modulator operating on the basis of a π-cell. The proposed method has an accuracy of modeling the characteristics of an LC modulator comparable to known analogue. The proposed simple method for calculating the transmission coefficient of the LC modulator, in contrast to the "classical" Abeles method, allows taking into account multi-beam interference in anisotropic layered media.

Based on the results of computer modeling, the following conclusions can be made:

1) The influence of changes in the design parameters on the transmission coefficient of the LC modulator increases with a decrease in the wavelength of the electromagnetic range within the range from 16 μm to 1 μm.
2) The maximum influence on the transmission coefficient of the LC modulator in the short-wave part of electromagnetic radiation is exerted by the thickness of the electrode layer, while in the long-wave part of this radiation there is no such dependence. The thickness of the orientation layer of the LC modulator has the same influence on its transmission coefficient as the thickness of the electrode layer, but with a smaller amplitude. The significant influence of the thickness of the electrode layer on the transmittance of the LC modulator is explained by the fact that the refractive index of this layer differs significantly from the refractive index of other elements of the modulator.
3) The control voltage of the LC modulator has a significant effect on its transmission coefficient of electromagnetic radiation for short wavelengths and has almost no effect on it in the long-wave region.

In the future, it is planned to search for the optimal design of a THz range LC modulator for different wavelengths of modulated radiation.

Ethical Statement

This study does not contain any studies with human or animal subjects performed by any of the authors.

Conflicts of Interest

The authors declare that they have no conflicts of interest to this work.

Data Availability Statement

Data are available from the corresponding author upon reasonable request.

Author Contribution Statement

Anfal Fadhil Ahmed Mulamahawsh: Validation, Formal analysis, Investigation, Writing – original draft, Visualization. **G. V. Simonenko:** Conceptualization, Methodology, Software, Validation, Formal analysis, Data curation, Writing – review & editing, Visualization, Supervision, Project administration.

References

[1] Lee, W., Han, S., Moon, S.-R., Park, J., Yoo, S., Park, H., ..., & Cho, S. H. (2022). Coherent terahertz wireless communication using dual-parallel MZM-based silicon photonic integrated circuits. *Optics Express*, *30*(2), 2547–2563. https://doi.org/10.1364/OE.446516

[2] Mu, T., Ye, Y., Dai, Z., Zhao, R., Yang, M., & Ren, X. (2022). Silver nanoparticles-integrated terahertz metasurface for enhancing sensor sensitivity. *Optics Express*, *30*(23), 41101–41109. https://doi.org/10.1364/OE.472520

[3] Lu, P.-K., Fernandez Olvera, A. D. J., Turan, D., Seifert, T. S., Yardimci, N. T., Kampfrath, T., ..., & Jarrahi, M. (2022). Ultrafast carrier dynamics in terahertz photoconductors and photomixers: Beyond short-carrier-lifetime semiconductors. *Nanophotonics*, *11*(11), 2661–2691. https://doi.org/10.1515/nanoph-2021-0785

[4] Sun, X., Lyu, Z.-H., Wu, H.-Z., Meng, C.-S., Zhang, D.-W., Lu, Z.-Z., ..., & Yuan, J.-M. (2022). Broadband terahertz detection by laser plasma with balanced optical bias. *Sensors*, *22*(19), 7569. https://doi.org/10.3390/s22197569

[5] Lin, Q.-W., Wong, H., Huitema, L., & Crunteanu, A. (2022). Coding metasurfaces with reconfiguration capabilities based on optical activation of phase-change materials for terahertz beam manipulations. *Advanced Optical Materials*, *10*(1), 2101699. https://doi.org/10.1002/adom.202101699

[6] Xu, F., Huang, X., Wu, Q., Zhang, X., Shang, Z., & Zhang, Y. (2022). YOLO-MSFG: Toward real-time detection of concealed objects in passive terahertz images. *IEEE Sensors Journal*, *22*(1), 520–534. https://doi.org/10.1109/JSEN.2021.3127686

[7] Peng, Z., Zheng, Z., Yu, Z., Lan, H., Zhang, M., Wang, S., ..., & Su, H. (2023). Broadband absorption and polarization conversion switchable terahertz metamaterial device based on vanadium dioxide. *Optics & Laser Technology*, *157*, 108723. https://doi.org/10.1016/j.optlastec.2022.108723

[8] Abdelraouf, O. A. M., Wang, Z., Liu, H., Dong, Z., Wang, Q., Ye, M., ..., & Liu, H. (2022). Recent advances in tunable metasurfaces: Materials, design, and applications. *ACS Nano*, *16*(9), 13339–13369. https://doi.org/10.1021/acsnano.2c04628

[9] Zeng, H., Gong, S., Wang, L., Zhou, T., Zhang, Y., Lan, F., ..., & Mittleman, D. M. (2022). A review of terahertz phase modulation from free space to guided wave integrated devices. *Nanophotonics*, *11*(3), 415–437. https://doi.org/10.1515/nanoph-2021-0623

[10] Wang, L., An, N., He, X., Zhang, X., Zhu, A., Yao, B., & Zhang, Y. (2022). Dynamic and active THz graphene metamaterial devices. *Nanomaterials*, *12*(12), 2097. https://doi.org/10.3390/nano12122097

[11] Hagras, E. A. A., Hameed, M. F. O., & Obayya, S. S. A. (2022). Compact dual-core liquid crystal photonic crystal fiber polarization splitter for terahertz applications. *Optik*, *265*, 169396. https://doi.org/10.1016/j.ijleo.2022.169396

[12] Li, J.-S., Li, S.-H., & Yao, J.-Q. (2020). Actively tunable terahertz coding metasurfaces. *Optics Communications*, *461*, 125186. https://doi.org/10.1016/j.optcom.2019.125186

[13] Sun, Y., Xu, Y., Li, H., Liu, Y., Zhang, F., Cheng, H., ..., & Wen, L. (2022). Flexible control of broadband polarization in a spintronic terahertz emitter integrated with liquid crystal and metasurface. *ACS Applied Materials & Interfaces*, *14*(28), 32646–32656. https://doi.org/10.1021/acsami.2c04782

[14] Guo, Q., Liu, T., Wang, X., Zheng, Z., Kudreyko, A., Zhao, H., ..., & Kwok, H.-S. (2020). Ferroelectric liquid crystals for fast switchable circular Dammann grating. *Chinese Optics Letters*, *18*(8), 080002. https://doi.org/10.3788/COL202018.080002

[15] Ji, Y., Jiang, X., Fan, F., Zhao, H., Cheng, J., Wang, X., & Chang, S. (2023). Active terahertz beam deflection based on a phase gradient metasurface with liquid crystal-enhanced cavity mode conversion. *Optics Express*, *31*(2), 1269–1281. https://doi.org/10.1364/OE.479856

[16] Khoo, I.-C. (2007). *Liquid crystals* (2nd ed.). USA: Wiley. https://doi.org/10.1002/0470084030

[17] Panchal, R., & Sinha, A. (2022). Low threshold optical attenuator based on electrically tunable liquid crystal cladding waveguide. *Optics Communications*, *513*, 128089. https://doi.org/10.1016/j.optcom.2022.128089

[18] Sharma, V., Sinha, A., & Shenoy, M. R. (2022). Mode size converter based on periodically segmented liquid crystal core waveguide. *Journal of Lightwave Technology*, *40*(14), 4728–4734. https://doi.org/10.1109/JLT.2022.3168573

[19] Tripathi, U. S., & Rastogi, V. (2020). Liquid crystal-based rib waveguide. *Journal of Lightwave Technology*, *38*(15), 4045–4051. https://doi.org/10.1109/JLT.2020.2985924

[20] Tripathi, U. S., Bijalwan, A., & Rastogi, V. (2020). Rib waveguide based liquid crystal EO switch. *IEEE Photonics Technology Letters*, *32*(23), 1453–1456. https://doi.org/10.1109/LPT.2020.3032876

[21] Tripathi, U. S., & Rastogi, V. (2019). Liquid crystal-based widely tunable integrated optic wavelength filters. *Journal of the Optical Society of America B*, *36*(7), 1883–1889. https://doi.org/10.1364/JOSAB.36.001883

[22] Lagerwall, J. P. F., & Scalia, G. (Eds.). (2017). *Liquid crystals with nano and microparticles* (Vol. 1). Singapore: World Scientific Publishing.

[23] Siarkowska, A., Chychłowski, M., Budaszewski, D., Jankiewicz, B., Bartosewicz, B., & Woliński, T. R. (2017). Thermo- and electro-optical properties of photonic liquid crystal fibers doped with gold nanoparticles. *Beilstein Journal of Nanotechnology*, *8*, 2790–2801. https://doi.org/10.3762/bjnano.8.278

[24] Abuabed, A. S. A. (2017). Study of the effect of nematic order degradation in liquid crystal-based surface plasmon resonance sensors. *Photonics*, *4*(2), 24. https://doi.org/10.3390/photonics4020024

[25] Turowski, B., & Rutkowska, K. A. (2017). Fabrication of liquid crystalline periodic waveguiding structures by means of the photo-polymerization process. *Photonics Letters of Poland*, *9*(3), 82–84. https://doi.org/10.4302/plp.v9i3.770

[26] Simonenko, G. V., & Mulamakhavsh, A. F. A. (2024). Modulyatsiya teragertsovogo izlucheniya s pomoshch'yu zhidkokristallicheskikh π-yacheyek [Modulation of terahertz radiation using liquid crystal π-cells]. *Applied Physics*, (3), 13–19.

[27] Yakovlev, D. A., Chigrinov, V. G., & Kwok, H.-S. (Eds.). (2015). *Modeling and optimization of LCD optical performance*. UK: Wiley. https://doi.org/10.1002/9781118706749

[28] Chigrinov, V., Podyachev, Y., Simonenko, G., & Yakovlev, D. (2000). The optimization of LCD electrooptical behavior using MOUSE-LCD software. *Molecular Crystals and Liquid Crystals Science and Technology. Section A. Molecular Crystals and Liquid Crystals*, *351*(1), 17–25. https://doi.org/10.1080/10587250008023248

[29] Azzam, R. M. A., & Bashara, N. M. (1977). *Ellipsometry and polarized light*. Netherlands: North-Holland Publishing Company.

[30] Bos, P. J., & Koehler-Beran, K. R. (1984). The pi-cell: A fast liquid-crystal optical-switching device. *Molecular Crystals and Liquid Crystals*, *113*(1), 329–339. https://doi.org/10.1080/00268948408071693

[31] Sevostianov, V. P., Simonenko, G. V., Brezhnev, V. A., Studentsov, S. A., & Yakovlev, D. A. (1997). Experimental and theoretical study of optical characteristics of LC shutter on π-cells. *Photonics and Optoelectronics*, *4*(4), 139–146.

[32] Born, M., & Wolf, E. (1964). *Principles of optics: Electromagnetic theory of propagation, interference and diffraction of light*. USA: Macmillan.

How to Cite: Mulamahawsh, A. F. A., & Simonenko, G. V. (2026). Dependence of the Electromagnetic Radiation Transmission Coefficient of Liquid Crystal π – Cells in the Terahertz Range. *Journal of Optics and Photonics Research*, *3*(2), 140–145. https://doi.org/10.47852/bonviewJOPR52025210